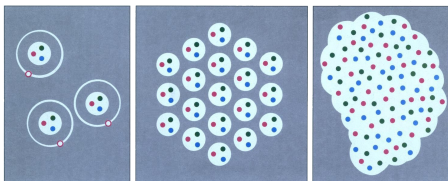


# New algorithms and new results for Strong Coupling LQCD

Wolfgang Unger, ETH Zürich  
with Philippe de Forcrand, ETH Zürich/CERN  
Lattice 2012, Cairns

26.06.2012



Eidgenössische Technische Hochschule Zürich  
Swiss Federal Institute of Technology Zurich

# 1 Motivation for Strong Coupling LQCD in Continuous Time

- Continuous Time Limit and  $a/a_t = f(\gamma)$
- Continuous Time Partition Function  $Z(\beta)$

# 2 Quantum Monte Carlo Methods

- Spin Representation
- Stochastic Series Expansion

# 3 Application: 2 flavor SC-LQCD

- Generalization of Spin Representation
- Preliminary Results

## Why Strong Coupling Lattice QCD?

Look at Lattice QCD in a regime where the finite baryon density **sign problem** can be made mild:

$$\beta = \frac{2N_c}{g^2} \rightarrow 0$$

- allows to integrate out the gauge fields completely, as **link integration factorizes**  
 $\Rightarrow$  no fermion determinant
- drawback: strong coupling limit is converse to asymptotic freedom, lattice is maximally coarse

Strong coupling LQCD shares important features with QCD:

- exhibits **confinement**, i.e. only color singlet degrees of freedom survive:
  - **mesons** (represented by monomers and dimers)
  - **baryons** (represented by oriented self-avoiding loops)
- and **spontaneous chiral symmetry breaking/restoration**: (restored at  $T_c$ )  
 $\Rightarrow$  SC-LQCD is a great laboratory to study the full  **$T-\mu$  phase diagram**

SC-LQCD is a useful toymodel for **nuclear matter**

## Why Strong Coupling Lattice QCD?

Look at Lattice QCD in a regime where the finite baryon density **sign problem** can be made mild:

$$\beta = \frac{2N_c}{g^2} \rightarrow 0$$

- allows to integrate out the gauge fields completely, as **link integration factorizes**  
 $\Rightarrow$  no fermion determinant
- drawback: strong coupling limit is converse to asymptotic freedom, lattice is maximally coarse

Strong coupling LQCD shares important features with QCD:

- exhibits **confinement**, i.e. only color singlet degrees of freedom survive:
  - **mesons** (represented by monomers and dimers)
  - **baryons** (represented by oriented self-avoiding loops)
- and **spontaneous chiral symmetry breaking/restoration**: (restored at  $T_c$ )  
 $\Rightarrow$  SC-LQCD is a great laboratory to study the full  **$T-\mu$  phase diagram**

SC-LQCD is a useful toymodel for **nuclear matter**

SC-LQCD is a **1-parameter deformation of QCD**

# SC-LQCD at finite temperature

How to vary the temperature?

- $aT = 1/N_\tau$  is discrete with  $N_\tau$  even
- $aT_c \simeq 1.5$ , i.e.  $N_\tau^c < 2 \Rightarrow$  we cannot address the phase transition!

**Solution:** introduce an **anisotropy**  $\gamma$  in the Dirac couplings:

$$\mathcal{Z}(m_q, \mu, \gamma, N_\tau) = \sum_{\{k, n, l\}} \prod_{b=(x, \mu)} \frac{(3 - k_b)!}{3! k_b!} \gamma^{2k_b \delta_{\mu 0}} \prod_x \frac{3!}{n_x!} (2am_q)^{n_x} \prod_l w(\ell, \mu)$$

Should we expect  $a/a_\tau = \gamma$ , as suggested at weak coupling?

- **No:** meanfield predicts  $a/a_\tau = \gamma^2$ , since  $\gamma_c^2 = N_\tau \frac{(d-1)(N_c+1)(N_c+2)}{6(N_c+3)}$

$\Rightarrow$  sensible,  $N_\tau$ -independent definition of the temperature:

$$aT \simeq \frac{\gamma^2}{N_\tau}$$

- Moreover, SC-LQCD partition function is a function of  $\gamma^2$

However: **precise correspondence between  $a/a_\tau$  and  $\gamma^2$  not known**

# SC-LQCD at finite Temperature and Continuous Time:

Strategy for **unambiguous** answer: the **continuous Euclidean time limit** (CT-limit):

$$N_\tau \rightarrow \infty, \quad \gamma \rightarrow \infty, \quad \gamma^2/N_\tau \equiv aT \text{ fixed}$$

- same as in analytic studies:  $a_\tau = 0$ ,  $aT = \beta^{-1} \in \mathbb{R}$

# SC-LQCD at finite Temperature and Continuous Time:

Strategy for **unambiguous** answer: the **continuous Euclidean time limit** (CT-limit):

$$N_\tau \rightarrow \infty, \quad \gamma \rightarrow \infty, \quad \gamma^2/N_\tau \equiv aT \text{ fixed}$$

- same as in analytic studies:  $a_\tau = 0$ ,  $aT = \beta^{-1} \in \mathbb{R}$

Several **advantages** of continuous Euclidean time approach:

- ambiguities arising from the functional dependence of observables on the anisotropy parameter will be circumvented, **only one parameter** setting the temperature
- no need to perform the continuum extrapolation  $N_\tau \rightarrow \infty$
- allows to estimate critical temperatures more precisely, with a faster algorithm (about 10 times faster than  $N_t = 16$  at  $T_c$ )
- baryons become static in the CT-limit, the **sign problem is completely absent!**

# Continuous Time Partition Function

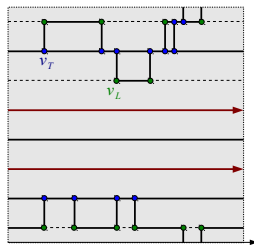
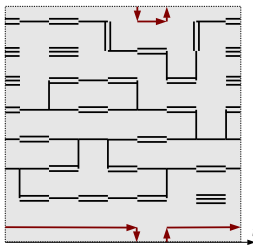
Partition function in the limit of large  $\gamma^2$ ,  $N_\tau$  with  $T = \gamma^2/N_\tau$ :

$$\mathcal{Z}(\gamma, N_\tau) = \sum_{\{k, n_B(x)\}} e^{3n_B \mu/T} \prod_{x \in V_M} \left(\frac{v_L}{\gamma}\right)^{n_L(x)} \left(\frac{v_T}{\gamma}\right)^{n_T(x)}, \quad n_B(x) \in \{-1, 0, 1\}$$

- $V_M \subseteq N_\sigma^3$  is mesonic subvolume and  $n_B = \sum_x n_B(x)$  is baryon number
- multiple spatial dimer become resolved into **single spatial dimers** as  $a_t \rightarrow 0$

typical (2-dimensional) configurations in discrete and continuous time at the same temperature:

- weight of configuration given by **number of spatial dimers and vertices** ( $v_L$ ,  $v_T$ ) **regardless of time coordinates**
- **baryons** become **static** in continuous time!





# Diagrammatic Partition Function

Rewrite partition function in inverse temperature  $\beta = 1/aT$ :

- sum over all spatial dimer time coordinantes  $\sim N_\tau/2 \Rightarrow$  **expansion in  $\beta = N_\tau/\gamma^2$**
- number of spatial dimers:  $\kappa = \frac{1}{2} \sum_{x \in V_M} (n_L(x) + n_T(x))$

$$\mathcal{Z}(\beta) = \sum_{\kappa \in 2\mathbb{N}} \frac{(\beta/2)^\kappa}{\kappa!} \sum_{\mathcal{C} \in \Gamma_\kappa} v_T^{n_T(\mathcal{C})} e^{\beta 3\mu B(\mathcal{C})}, \quad n_T = \sum_x n_T(x)$$

- $\Gamma_\kappa$  is the set of equivalence classes of configurations with  $\kappa$  spatial dimers, time coordinates of spatial dimers irrelevant

Importance sampling of diagrams described in terms of a perturbative series:

- each term  $\Gamma_\kappa$  is represented by a **world line configuration**
- perturbative series may not converge, but for any finite volume and temperature, only a finite number of orders contribute
- important QMC techniques: **continuous time worm** (Beard & Wiese), loop cluster algorithm (Evertz et al.), **stochastic series expansion** (Sandvik)

# Diagrammatic Partition Function

Rewrite partition function in inverse temperature  $\beta = 1/aT$ :

- sum over all spatial dimer time coordinantes  $\sim N_\tau/2 \Rightarrow$  **expansion in  $\beta = N_\tau/\gamma^2$**
- number of spatial dimers:  $\kappa = \frac{1}{2} \sum_{x \in V_M} (n_L(x) + n_T(x))$

$$\mathcal{Z}(\beta) = \sum_{\kappa \in 2\mathbb{N}} \frac{(\beta/2)^\kappa}{\kappa!} \sum_{C \in \Gamma_\kappa} v_T^{n_T(C)} e^{\beta 3\mu B(C)}, \quad n_T = \sum_x n_T(x)$$

- $\Gamma_\kappa$  is the set of equivalence classes of configurations with  $\kappa$  spatial dimers, time coordinates of spatial dimers irrelevant

Importance sampling of diagrams described in terms of a perturbative series:

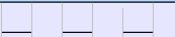



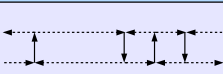



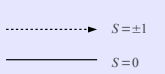
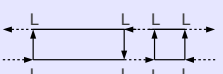

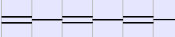
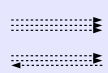
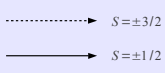
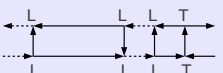
- each term  $\Gamma_\kappa$  is represented by a **world line configuration**
- perturbative series may not converge, but for any finite volume and temperature, only a finite number of orders contribute
- important QMC techniques: **continuous time worm** (Beard & Wiese), loop cluster algorithm (Evertz et al.), **stochastic series expansion** (Sandvik)

results for SC-LQCD obtained with CT-Worm algorithm reported last year  
(phase diagram in the  $\mu-T$  plane) [hep-lat/1111.1434]

# Mapping of 1-flavor $SU(N_c)$ to a spin system

Continuous time methods can be applied to any gauge group  $SU(N_c)$ :

- baryons become static for  $N_c \geq 3$
- mesonic discrete time chains **classified by parity:**

	Discrete Time Chains	Parity Composition	Spin Composition	Example Configuration
<b>U(1)</b>	<div> <i>even</i>  </div> <div> <i>odd</i>  </div>			
<b>U(2)</b>	<div> <i>ee/oo</i>  </div> <div> <i>eo</i>  </div>			
<b>U(3)</b>	<div> <i>eee/ooo</i>  </div> <div> <i>eeo/ooe</i>  </div>			

⇒ mesonic CT line types **classified by “spin”**:  $S = -N_c/2 \dots N_c/2$   
 (remnant of staggered even/odd ordering),  $\Delta S = \pm 1$  (absorption/emission)

- generalizes to arbitrary  $U(N_c)$

# Stochastic Series Expansion

Idea: rewrite partition function, based on decomposition in diagonal and non-diagonal elements  $\mathcal{H} = \mathcal{H}_1 + \mathcal{H}_2$ , truncation  $L$ :

$$\mathcal{Z}(\beta) = \text{Tr} \{ e^{-\beta \mathcal{H}} \} = \sum_{\chi} \sum_{S_L} \frac{\beta^{\kappa} (L - \kappa)!}{L!} \left\langle \chi \left| \prod_{i=1}^L \mathcal{H}_{a_i, b_i} \right| \chi \right\rangle, \quad \begin{aligned} \mathcal{H}_{1,b} &= \varepsilon \mathbb{1}, \varepsilon \geq 0 \\ \mathcal{H}_{2,b} &= \frac{1}{2} S_x^+ S_y^- \end{aligned}$$

with  $S_L$  a **time-ordered sequence** of operator-indices:  $S_L = [a_1, b_1], [a_2, b_2], \dots [a_L, b_L]$

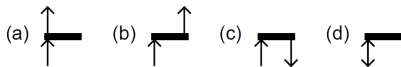
- $a_i = 0$ : identity,  $a_i = 1, 2$ : diagonal/non-diagonal matrix element
- $b_i = \langle x, y \rangle \in Vd$  denotes a bond

Two kinds of **updates**:

**1** **changing order in  $\beta$** ,  $\kappa \mapsto \kappa \pm 1$ :

$$P([1, b]_p \mapsto [0, 0]_p) = \frac{L - \kappa + 1}{Vd\beta \langle \chi | \mathcal{H}_{1,b} | \chi \rangle}, \quad P([0, 0]_p \mapsto [1, b]_p) = \frac{Vd\beta \langle \chi | \mathcal{H}_{1,b} | \chi \rangle}{L - \kappa}$$

**2** **operator loop**: visit bonds  $b_i$  successively from an input leg, determine output leg with heatbath probability  $\langle \chi_x \chi_y | \mathcal{H}_{a_i b_i} | \chi'_x \chi'_y \rangle$



$L$  is set larger than  $\kappa_{\max} \Rightarrow$  **SSE is approximation free** (like CT-Worm)

# SSE applied to SC-LQCD

Strong Coupling  $U(1)$  is identical to **XY Model** in zero field!

- new observable: spin susceptibility  $\chi_S = \beta \langle (\sum_i S_i^z)^2 \rangle / N$

Extension to  $U(3)$  for SC-LQCD straightforward:

$$\mathcal{H} = \frac{1}{2} \sum_{\langle x, y \rangle} J_x^+ J_y^-$$

$$\text{with } J^+ = \begin{pmatrix} 0 & & & \\ v_L & 0 & & \\ & v_T & 0 & \\ & & 0 & v_L \end{pmatrix}$$

and  $J^- = (J^+)^T$  for absorption/emission

- state vector characterizing time slice:  
 $|S^z\rangle(t) \in \left\{ \bigotimes_{\vec{x} \in V} S_{\vec{x}}^z \mid S_{\vec{x}}^z \in \{-N_c/2, \dots, N_c/2\} \right\}$
- oriented spatial dimers** act at time  $t_i$  on  $|S_x\rangle$  by raising/lowering spin at absorption/emission site
- lowest/highest weight:  $J^+ |N_c/2\rangle = 0, \quad J^- | -N_c/2\rangle = 0$
- $S^z$  counts net number of (odd-even) time like meson sites at each site
- $\frac{N_c}{2} [J^+, J^-] = J^z = \text{diag}(-N_c/2, \dots, N_c/2)$  fulfilled,  $J^z |S^z\rangle = S^z |S^z\rangle$

# SSE applied to SC-LQCD

Strong Coupling  $U(1)$  is identical to **XY Model** in zero field!

- new observable: spin susceptibility  $\chi_S = \beta \langle (\sum_i S_i^z)^2 \rangle / N$

Extension to  $U(3)$  for SC-LQCD straightforward:

$$\mathcal{H} = \frac{1}{2} \sum_{\langle x, y \rangle} J_x^+ J_y^-$$

$$\text{with } J^+ = \begin{pmatrix} 0 & & & \\ v_L & 0 & & \\ & v_T & 0 & \\ & & 0 & v_L \end{pmatrix}$$

and  $J^- = (J^+)^T$  for absorption/emission

- state vector characterizing time slice:  
 $|S^z\rangle(t) \in \left\{ \bigotimes_{\vec{x} \in V} S_{\vec{x}}^z \mid S_{\vec{x}}^z \in \{-N_c/2, \dots, N_c/2\} \right\}$
- oriented spatial dimers** act at time  $t_i$  on  $|S_x\rangle$  by raising/lowering spin at absorption/emission site
- lowest/highest weight:  $J^+ |N_c/2\rangle = 0, \quad J^- | -N_c/2\rangle = 0$
- $S^z$  counts net number of (odd-even) time like meson sites at each site
- $\frac{N_c}{2} [J^+, J^-] = J^z = \text{diag}(-N_c/2, \dots, N_c/2)$  fulfilled,  $J^z |S^z\rangle = S^z |S^z\rangle$

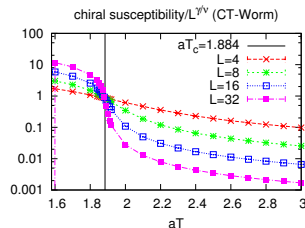
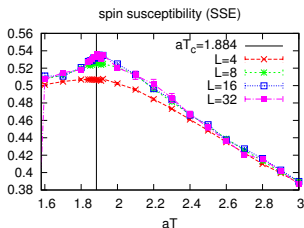
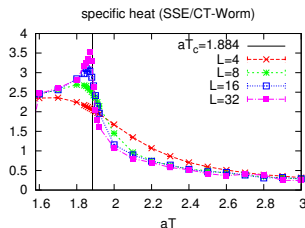
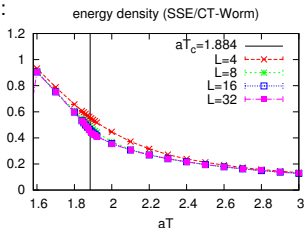
“Spin” is a conserved quantity, generalizes for arbitrary  $N_c$ !

# Comparison of Continuous Time Worm and SSE

Observables in both algorithms: energy, specific heat (obtained from # spatial dimers)

- CT-Worm faster if truncation  $L$  is unlimited in SSE
- SSE faster if  $L$  is fixed and not too large

$N_c = 3$ :

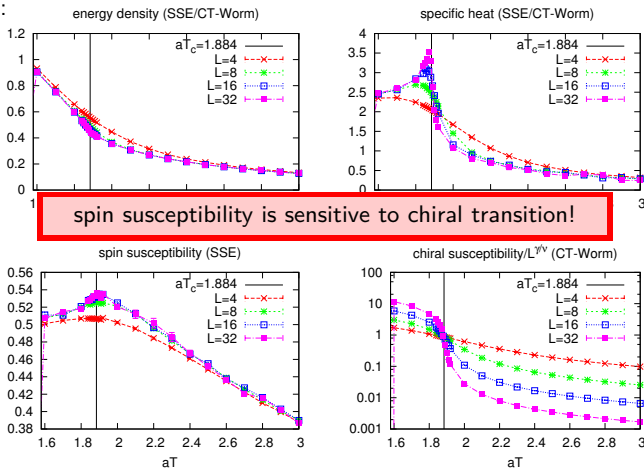


# Comparison of Continuous Time Worm and SSE

Observables in both algorithms: energy, specific heat (obtained from # spatial dimers)

- CT-Worm faster if truncation  $L$  is unlimited in SSE
- SSE faster if  $L$  is fixed and not too large

$N_c = 3$ :

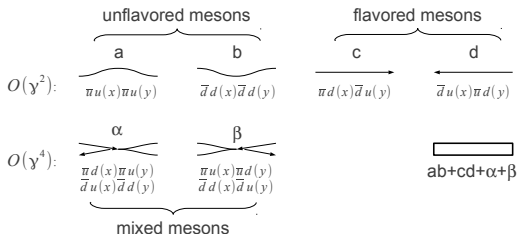




# Application: Generalization of SC-LQCD to 2 chiral flavors!

Aim: obtain phase diagram for 2-flavor SC-LQCD, where **pion exchange** may play a crucial role for nuclear transition, but:

- at present, no 2-flavor formulation for staggered SC-LQCD suitable for MC
- already the mesonic sector has a severe **sign problem** (worse than for finite  $\mu$  HMC)
- 2 new types of mixed dimers give negative sign in mesonic loops already for  $U(2)$ :



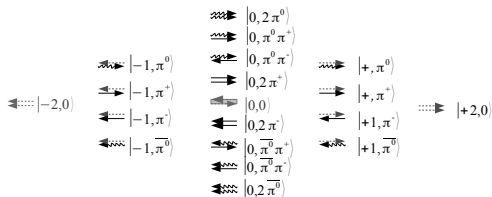
Observation in continuous time formulation:

- **static lines** for 2 different flavors can be composed such that **cancellations appear**
- first step in this direction: use SSE (simpler than CT-Worm)

## Continuous Time Transition Rules

Flavored static lines:

- new classification in terms of **quantum numbers**  
 $|S^z, Q_{\pi^0}, Q_{\pi^+}\rangle$
- in total: 19 types of lines, 18 have weight  $1/16$  per  $2a_t$ ,  
 “vacuum state”  $|0, 0, 0\rangle$  has weight  $1/8$



Quantum Numbers:

- “spin”  $S^z$  counts number of emission/absorption events (remnant of even/odd decomposition of lattice for staggered fermions)  $S^z = -\frac{1}{2} N_c N_f, \dots, +\frac{1}{2} N_c N_f$
- “charges”  $Q_i = -N_c, \dots, +N_c$  denote the flavor content
- **spin/charge conservation:** transitions at spatial dimers, raising charges at one site, lowering at a neighboring site:

$$|\Delta S^z| = 1, \quad |\Delta Q_{\pi^0}| + |\Delta Q_{\pi^+}| = 1$$

# Hamiltonian for $N_f = 2$ , $N_c = 2$

$$\mathcal{H} = \frac{1}{2} \sum_{\langle x, y \rangle} \left( J_{\pi^0(x)}^+ J_{\pi^0(y)}^- + J_{\bar{\pi}^0(x)}^+ J_{\bar{\pi}^0(y)}^- + J_{\pi^+(x)}^+ J_{\pi^+(y)}^- + J_{\pi^+(x)}^+ J_{\pi^-(y)}^- \right)$$

Absorption ( $J_{\pi_i}^+$ , lower left triangle) and Emission ( $J_{\pi_i}^-$ , upper triangle), state vector

$$J_{\pi_i}^{+/-} = \begin{pmatrix} \begin{array}{c|c|c|c} \pi^0 & \bar{\pi}^0 & \pi^+ & \pi^- \\ \hline \pi^0 & & & \\ \hline \bar{\pi}^0 & & & \\ \hline \pi^+ & & & \\ \hline \pi^- & & & \end{array} & \begin{array}{c|c|c|c} & & & \\ \hline & \pi^0 & & \\ \hline & \bar{\pi}^0 & & \\ \hline & \pi^+ & & \\ \hline & \pi^- & & \end{array} & \begin{array}{c|c|c|c} & & \hat{\pi}^0 & \hat{\pi}^+ & \hat{\pi}^- \\ \hline & & \hat{\pi}^0 & \hat{\pi}^+ & \hat{\pi}^- \\ \hline & \pi^+ & \hat{\pi}^+ & \hat{\pi}^0 & \\ \hline & \pi^- & \hat{\pi}^- & \hat{\pi}^0 & \hat{\pi}^0 \end{array} & \\ \hline \begin{array}{c|c|c|c} & & & \\ \hline & \pi^0 & & \\ \hline & \bar{\pi}^0 & & \\ \hline & \pi^+ & & \\ \hline & \pi^- & & \end{array} & \begin{array}{c|c|c|c} & & & \\ \hline & & & \\ \hline & & & \\ \hline & & & \\ \hline & & & \end{array} & \begin{array}{c|c|c|c} & & & \\ \hline & & & \\ \hline & & & \\ \hline & & & \\ \hline & & & \end{array} & \begin{array}{c|c|c|c} & & & \\ \hline & & & \\ \hline & & & \\ \hline & & & \\ \hline & & & \end{array} \end{pmatrix}, \quad \chi = \begin{pmatrix} -2, 0 \\ -1, \pi^0 \\ -1, \bar{\pi}^0 \\ -1, \pi^+ \\ -1, \pi^- \\ 0, 2\pi^0 \\ 0, 2\bar{\pi}^0 \\ 0, 2\pi^+ \\ 0, 2\pi^- \\ -0, 2\pi^- \\ -0, 0 \\ -0, \pi^0 \pi^+ \\ 0, \pi^0 \pi^- \\ 0, \bar{\pi}^0 \pi^+ \\ 0, \bar{\pi}^0 \pi^- \\ 0, \pi^0 \pi^- \\ +1, \pi^0 \\ +1, \bar{\pi}^0 \\ +1, \pi^+ \\ +1, \pi^- \\ +2, 0 \end{pmatrix}$$

The vertex weights are  $v_{\pi_i} = 1$  for vertices not mixing the two charges  $Q_i$ , and  $v_{\hat{\pi}_i} = \frac{1}{\sqrt{2}}$  for vertices mixing the charges

## Hamiltonian for $N_f = 2, N_c = 2$

$$\mathcal{H} = \frac{1}{2} \sum_{\langle x, y \rangle} \left( J_{\pi^0(x)}^+ J_{\pi^0(y)}^- + J_{\bar{\pi}^0(x)}^+ J_{\bar{\pi}^0(y)}^- + J_{\pi^+(x)}^+ J_{\pi^+(y)}^- + J_{\pi^+(x)}^+ J_{\pi^-(y)}^- \right)$$

Absorption ( $J_{\pi i}^+$ , lower left triangle) and Emission ( $J_{\pi i}^-$ , upper triangle), state vector

$$J_{\pi^+}^{+/-} = \left( \begin{array}{c|c|c|c|c|c} \pi^+ & & \hat{\pi}^+ & & & \\ \hline & \pi^+ & & \pi^+ & \hat{\pi}^+ & \\ \hline & & \pi^+ & & & \\ \hline \pi^+ & & & & & \\ \hline & \hat{\pi}^+ & \pi^+ & & & \pi^+ \\ \hline & & & & \pi^+ & \\ \hline & \hat{\pi}^+ & & \hat{\pi}^+ & & \\ \hline & & \pi^+ & \pi^+ & & \\ \hline & & & & \pi^+ & \pi^+ \end{array} \right), \quad \chi = \left( \begin{array}{c} -2, 0 \\ \hline -1, \pi^0 \\ -1, \bar{\pi}^0 \\ -1, \pi^+ \\ -1, \pi^- \\ \hline 0, 2\pi^0 \\ 0, 2\bar{\pi}^0 \\ 0, 2\pi^+ \\ 0, 2\pi^- \\ \hline -0, 2\pi^- \\ -0, 0 \\ \hline -0, \pi^0 \pi^+ \\ -0, \pi^0 \pi^- \\ 0, \pi^0 \pi^+ \\ 0, \bar{\pi}^0 \pi^+ \\ 0, \bar{\pi}^0 \pi^- \\ \hline +1, \pi^0 \\ +1, \bar{\pi}^0 \\ +1, \pi^+ \\ +1, \pi^- \\ \hline +2, 0 \end{array} \right)$$

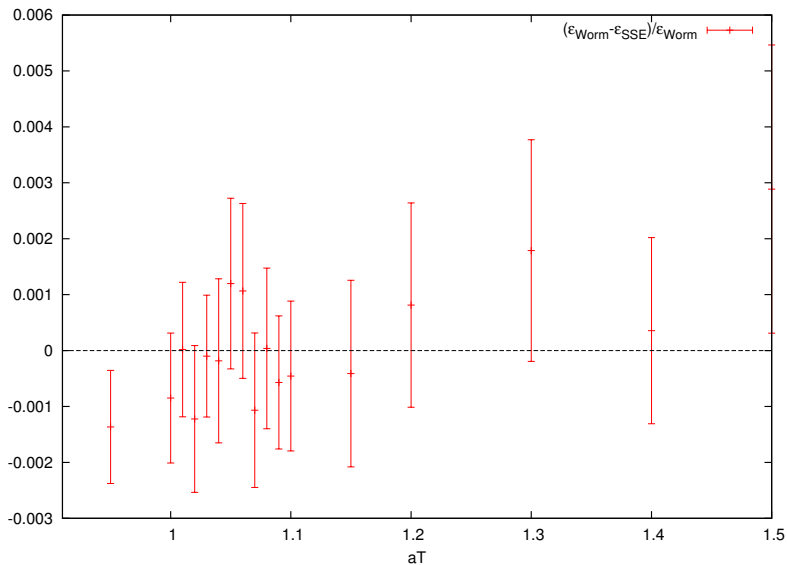
The vertex weights are  $v_{\pi_i} = 1$  for vertices not mixing the two charges  $Q_i$ , and  $v_{\hat{\pi}_i} = \frac{1}{\sqrt{2}}$  for vertices mixing the charges

# Conclusions

## Achievements:

- CT partition function: new formulation as a **spin system!**
- “spin” formulation and Hamiltonian follow from conservation laws for even/odd chains of time-like dimers and flavors - this **generalizes to arbitrary  $N_c, N_f$**
- new observable: spin susceptibility, sensitive to chiral transition
- quantum Monte Carlo applicable: e.g. continuous time worm or **stochastic series expansion** (most convenient)
- now also applied to  $U(2)$  with two flavors (incorporates pion exchange)
- extension to  $SU(3)$  with finite baryon chemical potential straightforward (Hamiltonian worked out, but no simulations yet)

# Comparison of SSE and CT-Worm



# SC-QCD Phase Diagram

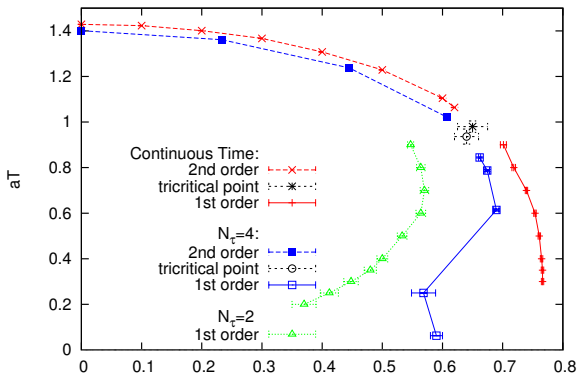
Studied via CT-Worm algorithm: arXiv:1111.1434 [hep-lat]

Comparison of phase diagram with  $N_\tau = 4$  data (M. Fromm, 2010):

- CT-data compared to  $N_\tau = 4$  data for identification

$$a\mu = \gamma^2 a_\tau \mu$$

- behavior at low  $\mu$  agrees well, location of TCP agrees within errors
- no re-entrance is seen at small temperatures

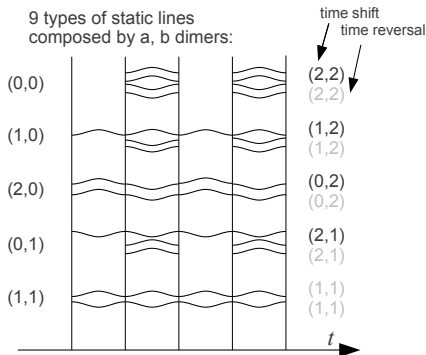


# Static Line Rules

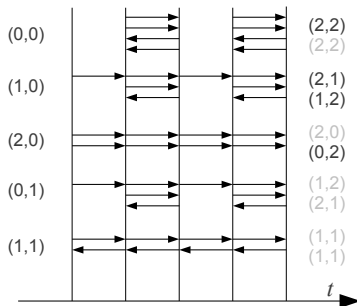
Combine temporal dimers of alternating orders in  $\gamma^2$  (here for  $N_c = 2$ ):

- first: consider  $(a, b)$  and  $(c, d)$  dimers separately
- then: resum them to obtain flux representation

9 types of static lines  
composed by a, b dimers:



9 types of static lines  
composed by c, d dimers:



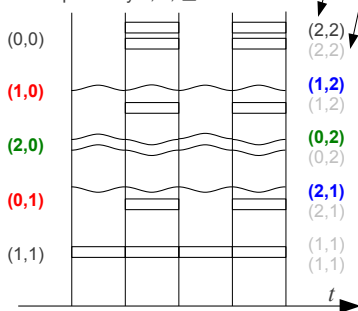


# Static Line Rules

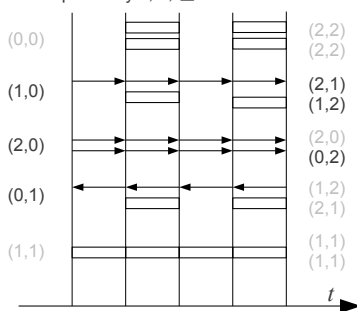
Combine temporal dimers of alternating orders in  $\gamma^2$  (here for  $N_c = 2$ ):

- resummation of  $a - b - a$  and  $b - a - b$  chains
- resummation of  $ab + cd + \alpha + \beta$  into  $\square$  dimers

9 types of static lines  
composed by a, b,  $\square$  dimers



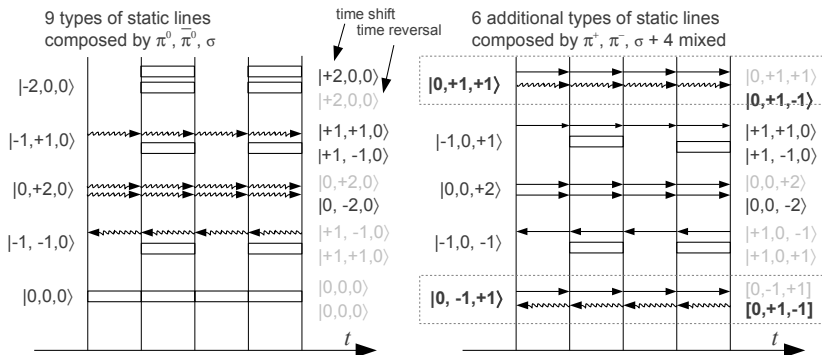
6 additional types of static lines  
composed by c, d,  $\square$  dimers



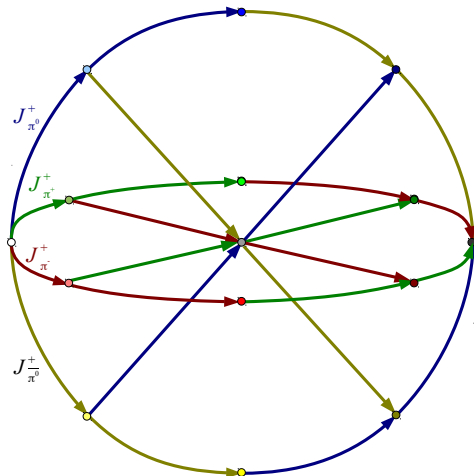
# Static Line Rules

Combine temporal dimers of alternating orders in  $\gamma^2$  (here for  $N_c = 2$ ):

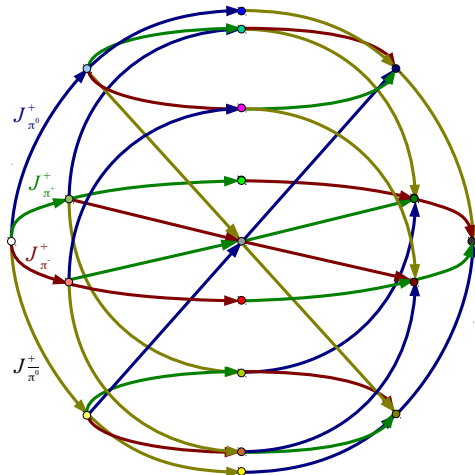
- new classification in terms of **quantum numbers**  $|S^z, Q_{\pi^0}, Q_{\pi^+}\rangle$
- in total: 19 types of lines, 18 have weight  $1/16$  per  $2a$ ,  $|0,0,0\rangle$  has weight  $1/8$



# The Transition Rules Encoded in $J^\pm$



# The Transition Rules Encoded in $J^\pm$



# Why Study Strong Coupling QCD on the Lattice?

Two possible scenarios for the relation between SC-LQCD (back) and the (L)QCD phase diagram for four flavors (front):

